SSP-based land use change scenarios: a critical uncertainty in future regional climate change projections

Melissa S. Bukovsky[1], Jing Gao[2], Linda O. Mearns[1], Brian C. O'Neill[3]

[1] Regional Integrated Sciences Collective, Computational and Information Systems Laboratory and Research Applications Laboratory, National Center for Atmospheric Research, Boulder, CO 80301, USA

[2] Department of Geography and Spatial Sciences & Data Science Institute, University of Delaware, Newark, DE 19716, USA

[3] Pardee Center for International Futures & Josef Korbel School of International Studies, University of Denver, Denver, CO 80208, USA.

Corresponding author: Melissa S. Bukovsky (bukovsky@ucar.edu)

ORCID iDs:
Bukovsky: https://orcid.org/0000-0001-6415-965X
Gao: https://orcid.org/0000-0003-1778-8909
Mearns: https://orcid.org/0000-0002-2875-5830
O'Neill: https://orcid.org/0000-0001-7505-8897

Author Contributions:
Conceptualization: All authors
Formal Analysis: Bukovsky, Gao
Funding acquisition: Mearns, O'Neill
Investigation: Bukovsky, Gao
Methodology: All authors
Software: Bukovsky, Gao
Visualization: Bukovsky
Writing – original draft: Bukovsky
Writing – review & editing: All authors

Submitted to Earth's Future: 26 August 2020

Key Points

1. Regional climate change projections of temperature and precipitation are strongly influenced by urban and agricultural land-use changes.
2. Different SSP-based land-use changes produce different climate changes.
3. Urban land expansion (SSP5) has a greater influence on CONUS climate change projections than agricultural land expansion (SSP3) under RCP8.5.

Abstract

We assess the combined effects of greenhouse-gas (GHG)-forced climate change and land-use changes (LUC) on regional climate projections. To do so, we produced regional climate model (RCM) simulations that are complementary to the North-American Coordinated Regional Downscaling Experiment (NA-CORDEX) simulations, but with future LUCs that are consistent with particular Shared Socioeconomic Pathways (SSPs) and related to a specific Representative Concentration Pathway (RCP), allowing us to assess the influence of the LUCs on RCM projections through the SSP+RCP scenarios framework.

We examine the state of the climate at the end of the 21st Century with and without two urban and agricultural LUC scenarios that follow SSP3 and SSP5 using the Weather Research and Forecasting model (WRF) forced by one global climate model under the RCP8.5 scenario. We find that LUCs following different societal trends under the SSPs can significantly affect climate projections in different ways.

In regions of significant cropland expansion into previous forest, projected annual mean temperature increases are diminished by around 0.5-1.0°C. Where urbanization is high, projected temperature increases are magnified, particularly in summer where projections are up to 4-5°C greater and minimum and maximum temperature projections are increased by 2.5-6°C, amounts that are on par with the warming due to GHG-forced climate change. Warming is also enhanced in the urban surroundings. Future urbanization also has a large influence on precipitation projections during the warm-season, increasing storm intensity, event length, and the overall amount over urbanized areas, and decreasing precipitation in surrounding areas.

Keywords: CORDEX, SSP, land use change, regional climate

Index terms: 1632 Land cover change, 1637 Regional climate change (4321), 3355 Regional modeling (4316), 3354 Precipitation (1854), 4321 Climate impact (1630, 1637, 1807, 8408)

Plain Language Summary

In many regional climate change studies, projections of future climate conditions are produced assuming the current spatial distribution of different land covers (e.g. urban, cropland, forest, etc.) will stay the same, even for long-term futures. In doing so, they neglect potential impacts of human land use changes on regional climate, and miss the opportunity to identify potential land use strategies that could moderate felt climate change effects. In this study, we model urban and agricultural land use changes (LUCs) following two pathways with different social and environmental trends throughout the 21st Century, and investigate how the LUCs might affect climate change in North America.

We find that future LUCs can strongly influence projections of temperature and precipitation. Generally, urban land expansion casted a larger impact than agricultural land expansion. In areas where croplands replace forests, the temperature increase caused by greenhouse gas warming is reduced, while in and near future urban areas, the temperature increase caused by greenhouses gas warming is doubled by warming effects from urban land expansion. Meanwhile, urban expansion enhances precipitation over urbanized areas making rainfall events heavier and longer, while precipitation in the surrounding areas is reduced.

1 Introduction

To date, many regional climate model (RCM) or limited-area modeling studies have focused on idealized land-use changes (LUCs), where entire land-cover types are removed, added, and/or replaced, to examine their effect on weather, climate, or climate change (e.g. Argüeso et al., 2016; Belušić et al., 2019; Davin et al., 2019; Gálos et al., 2011; Huber et al., 2014; Tölle et al., 2018). Few have gone further into more realistic or societally-informed assessments, and examined the effect of future policy-driven land-use change scenarios and their combined effect on climate change in RCM projections. In one recent example, one of few that we know of, Berkmans et al. (2019) used a European policy-based LUC scenario in an RCM to examine the LUC effect on climate relative to greenhouse-gas (GHG) forced climate change for the near-future, and showed a clear influence of the LUC on temperature. Another, Yilmaz et al. (2019), used ongoing and near future infrastructure projects and their effect on local land-use to examine the influence of expanded irrigation on the local water budget, finding a large climatological and potentially large societal impact. In some instances, RCM projections have been used to inform climate change impacts assessments including implied land-use changes using integrated assessment models, but have not incorporated the LUC into the RCMs (e.g., Harrison et al., 2019). These existing studies leave a gap in the assessment of plausible future LUCs and their effects on future climate in regional simulations.

We attempt to narrow this gap using LUC scenarios that are consistent with different Shared Socioeconomic Pathway (SSPs) in RCM simulations to assess the combined effects of greenhouse-gas-induced climate change and scenario-based anthropogenic LUCs on regional climate projections. More specifically, we examine the influence of the LUCs that underlie the combined Shared Socioeconomic Pathway (SSP)+Representative Concentration Pathway (RCP) framework using simulations produced for the North-American Coordinated Regional Downscaling Experiment (NA-CORDEX) and complementary simulations produced for this assessment that incorporate SSP-based LUC. We aim to answer the question, “Does inclusion of SSP-based LUCs modulate the regional climate model (RCM) projections significantly?”, as the answer to this simple question may have implications for future modeling efforts, as we will discuss.

As global model simulations produced for Phase 6 of the Coupled Model Intercomparison Project (CMIP6) as a part of the Scenario Model Intercomparison Project

(ScenarioMIP; O'Neill et al., 2016) incorporate SSP-based LUC scenarios related to RCP-based future emissions, exploring the effect of SSP-based LUCs in RCMs is highly relevant for informing future downscaling efforts that make use of ScenarioMIP simulations. This is particularly true for large-scale coordinated efforts like CORDEX, making our effort timely as well. Existing NA-CORDEX simulations hold land surface cover constant at present day conditions, which is typical in most, if not all, existing CORDEX simulations globally, while SSP-consistent projections anticipate potentially substantial changes in anthropogenic land use amounts and patterns. For example, Gao & O'Neill (2020) found the global total amount of urban land can increase by 6 fold by 2100, and economically developed regions (e.g. North America) experience comparable amounts of new urban land development to developing regions. All accentuate the need for investigations like ours.

Understanding the magnitude of the regional climate effects of LUC is additionally important to the SSP+RCP scenarios framework (O'Neill et al., 2019), in particular the assumption that climate model simulations that include a particular land use scenario are a reasonable representation of climate outcomes in scenarios with the same greenhouse gas forcing but a different land use scenario (O'Neill et al., 2016). Some results with global climate and land use models challenge this assumption (Jones et al., 2013) and multi-model experiments are underway to further test it (Lawrence et al., 2016), but in general it is an understudied problem. This work helps address this question, and will help inform thinking about possible needed modifications to the scenarios framework to better account for climate-land use interactions.

2 Methods

2.1 Description of SSPs and SSP-Consistent Land-Use Changes

We use SSPs 3 and 5 in this study, because together they span the range of uncertainties in both urban and agricultural land use in the U.S. over the coming decades. Here, agricultural land includes crop and pasture, but not managed forest. Under SSP3, countries generally focus on domestic issues due to increasing nationalism. Economic development is slow, and countries focus on energy and food security. Population growth is low in industrialized countries but high in developing countries. As such, the U.S. sees an increase in domestic cropland but low population growth, which translates to low urban land expansion. Under SSP5, the global economy grows quickly driven by material-intensive development and fossil fuel exploitation.

Global population growth is low overall compared to many other SSPs, but in the U.S. and other high-income countries, the population grows rapidly under a strong globalized economy. As a result, the U.S. sees a large amount of urban land expansion and a minimal increase in domestic cropland. Pastureland area decreases slightly in both scenarios. For more detail on the SSP narratives see O'Neill et al. (2017).

Interestingly, these two scenarios also provide great contrast in our simulations. Because SSP3 experiences primarily cropland expansion and SSP5 primarily urban land expansion, our simulations can isolate the effects of these two different types of land use change. Note that SSP3 usually does not reach the radiative forcing of RCP8.5 in integrated assessment models, as SSP5 does (Riahi et al., 2017). In this study we use a cropland projection from a variant of SSP3 developed to ensure consistency with the radiative forcing levels in RCP8.5. This "High Growth" variant of SSP3 (SSP3HG) includes modestly higher GDP growth that increases emissions and also agricultural land use relative to SSP3, without changing its basic nature (Ren et al., 2018). The urban land projection is based on the original SSP3; the effect of the higher GDP growth on this low urban land development scenario would be small.

The land-use changes (LUCs) consistent with the two SSPs were produced using two land-use models (LUMs). For urban land change, we use a newly-developed empirically-grounded model that produces realistic spatial and temporal patterns for long-term urban land change under different SSPs at a ⅛ degree resolution (Gao & O'Neill, 2019, 2020). For agricultural land change, the projections (Ren et al., 2018) were produced with an agricultural land use model at a ½ degree resolution (Meiyappan et al., 2014). The two independently produced types of land use were combined by giving preference to urban development, which implicitly assumes urban land use would win if it competes with agricultural uses for the same land.

2.2 WRF

This study leverages 25-km resolution Weather Research and Forecasting (WRF) (Skamarock et al., 2005) model simulations that were produced for NA-CORDEX to save on computational costs (Mearns et al., 2017). Specifically, we use the simulations forced by the MPI-ESM-LR GCM. This GCM has a mid-range equilibrium climate sensitivity relative to the full set of Coupled Model Intercomparison Program Phase 5 (CMIP5) simulations, and it provides relatively high quality boundary conditions for WRF (Bukovsky & Mearns, 2020; Rendfrey et al., 2018). The future climate follows RCP8.5 (Moss et al., 2010). The NA-CORDEX WRF configuration uses the Noah land-surface model to parameterize land surface processes and the United States Geological Survey (USGS) land-use categories listed in Table 1. Land-use is held constant throughout the entire simulation, and from the historical to the future climate. The simulation domain with the dominant baseline land-use type for each grid box is shown in Figure 1. The urban environment is represented in WRF simply as a type of surface cover with specific properties related to albedo, roughness, moisture, etc. Other configuration settings may be found on the NA-CORDEX website (Mearns et al., 2017; https://na-cordex.org/rcm-characteristics.html).

In order to assess the combined effects of the RCP8.5 GHG-induced climate change and future anthropogenic land-use change, complementary simulations with the same WRF configuration as used in NA-CORDEX were produced for 2075-2100 with prescribed land-use changes that are consistent with SSP3 and SSP5. Future land-use changes representing the decade starting at 2090 were prescribed for the entire 2075-2100 timeslice in the complementary simulations. As the NA-CORDEX simulations are transient simulations that cover 1950-2100, in order to guarantee an identical simulation initiation state, the new simulations were started using a restart file from the original NA-CORDEX simulation, but with modified land-use relevant variables, at July 1, 2073 (allowing a 1.5 year spin-up for the simulation to adjust to the new land-use state, which was removed for analysis).

Herein, the future simulations from NA-CORDEX that do not include the SSP-based LUCs are referred to as the no-LUC scenario and labeled as RCP8.5 only in figures, while the complementary future simulations with SSP-based LUCs applied are referred to as either SSP3+RCP8.5 or SSP5+RCP8.5.

Table 1. USGS land-use categories used in WRF.

Land-use Index	Land-use Category Description
1	Urban and Built-up Land
2	Dryland Cropland and Pasture
3	Irrigated Cropland and Pasture
4	Mixed Dryland/Irrigated Cropland and Pasture
5	Cropland/Grassland Mosaic
6	Cropland/Woodland Mosaic
7	Grassland
8	Shrubland
9	Mixed Shrubland/Grassland
10	Savanna
11	Deciduous Broadleaf Forest
12	Deciduous Needleleaf Forest
13	Evergreen Broadleaf
14	Evergreen Needleleaf
15	Mixed Forest
16	Water Bodies
17	Herbaceous Wetland
18	Wooden Wetland
19	Barren or Sparsely Vegetated
20	Herbaceous Tundra
21	Wooded Tundra
22	Mixed Tundra
23	Bare Ground Tundra
24	Snow or Ice

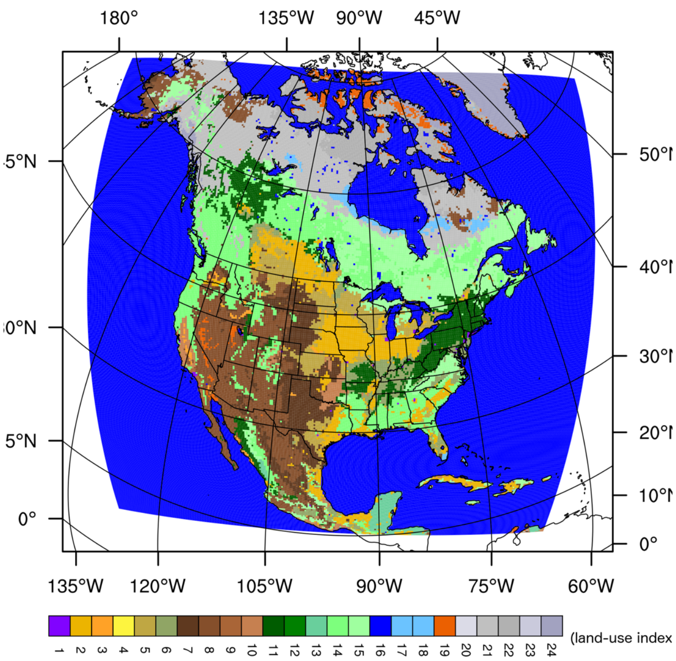

Figure 1. Simulation domain including the dominant land-use category from the baseline simulation for each WRF grid cell (see Table 1 for land-use index definition).

2.3 Application of LUC in WRF

Crop, pasture, and urban fractional land-cover fields from the historical period LUMs are not the same as their respective USGS/WRF counterparts in magnitude or spatial distribution, and in WRF, crop and pasture are represented by multiple land cover categories. Therefore, future changes in land use from the LUMs could not be directly applied in WRF. In WRF using the USGS land categories, cropland is represented in categories 2-6 in Table 1, and pasture, i.e. land that is suitable for grazing, could easily be seen as types 5, and 7-10. For this study, we applied the LUM changes as absolute fractional LUC deltas (LUM future minus LUM historical period land cover fraction) to types 2 or 3 for crop, using type 3 (irrigated crop) if it already existed as the predominant crop type in a grid box; pasture was applied to grassland category 7, and urban was applied to the urban land category 1. Also, total changes across the domain in the fractional land-use type fields for WRF were adjusted to be within 5% of those projected by the LUMs before application. New dominant land-use category fields, the field used in the Noah land-surface parameterization, were calculated from the adjusted land-use fraction fields. Further details regarding the application of the LUC can be found in the Supporting Information in Text S1. Historical, future, and individual change fields for crop, pasture, and urban land fraction from the LUMs and the modified categories in WRF are also provided in the Supporting

Information in Figures S1-S3 for reference. Changes in the dominant land category in each grid box in WRF are provided in Figure 2. Changes in the crop, pasture, and urban fractional fields as applied in WRF are summarized in Figure 3, and the percent of the total area each field represents over CONUS is given in Table 2a.

Figure 3 also indicates urban-rural point pairs that are used for analysis in Section 3. Each pair of points represents an urban point and an eastward/downwind (at least in winter) rural point (or at least less urban). Urban points in Figure 3 from west-to-east across the domain indicate the Portland, OR metropolitan area (PDX), the Dallas/Fort Worth, TX metroplex (DFW), the Minneapolis/St. Paul, MN metropolitan area (MSP), the Chicago, IL metropolitan area (CHI), the central Florida megaregion centered on Tampa (FL), and the Northeast Megalopolis centered on New Jersey (NJ).

Note that LUCs were only applied over the U.S., as plotted in Figure 3, as sub-country level crop and pasture projections could not be produced over the other countries in the domain due to the unavailability of historical crop and pasture data at sub-country level scales. Therefore, the presentation of our results will focus on the contiguous U.S. (CONUS), where the results of the application of LUC on the climate are the most relevant.

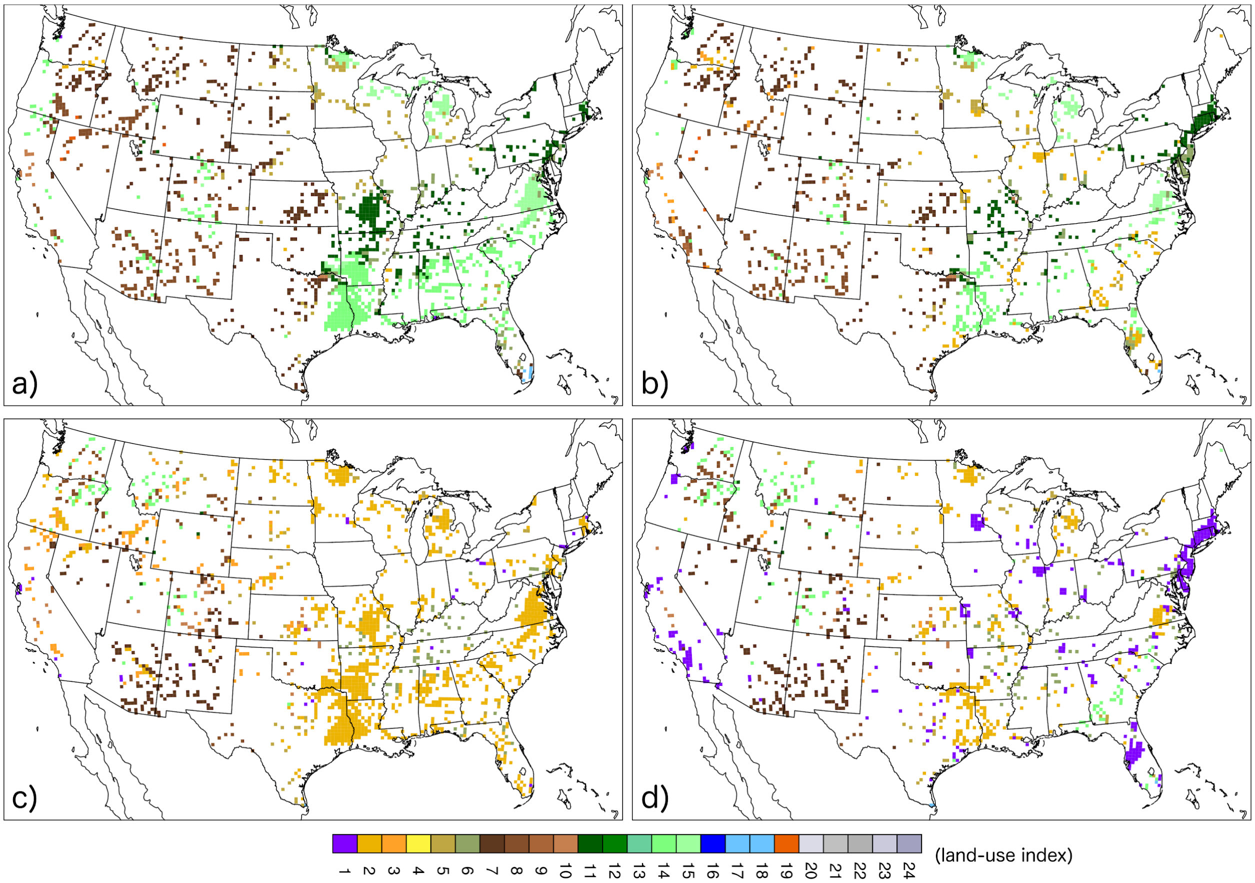

Figure 2. Dominant land-use category for only grid cells that end up changing category under an SSP-based LUC scenario, all others remain white (see Table 1 for land-use index definition). a) Category used in the historical and no-LUC simulations for cells that do change under SSP3+RCP8.5; b) as in a), but for cells that change under SSP3+RCP8.5; c) category under SSP3+RCP8.5; d) category under SSP5+RCP8.5.

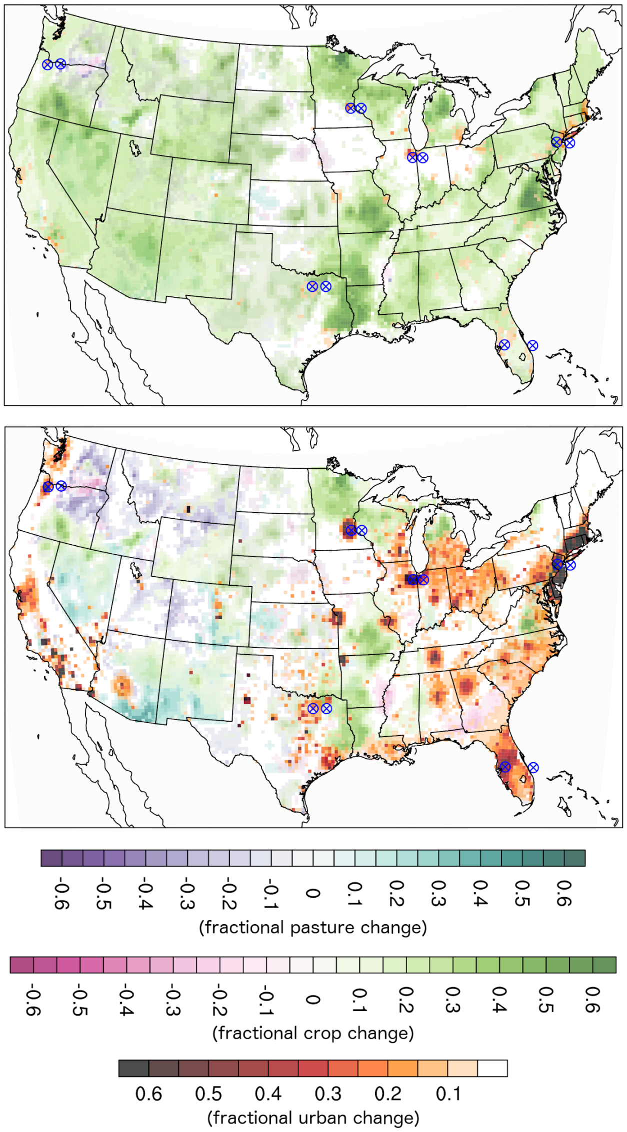

Figure 3. Absolute change in fractional land use from the baseline to the future in WRF under SSP3+RCP8.5 (top) and SSP5+RCP8.5 (bottom). Blue symbols indicate locations of point pairs used in our analysis, as described in Section 2.3. Fields are plotted at 70% opacity so strong changes in multiple fields at a given point can be identified. Urban change is plotted over crop change, which is plotted over pasture change.

Table 2. For the historical (hist), RCP8.5 no-LUC future (noLUC), SSP3+RCP8.5 future (SSP3), and SSP5+RCP8.5 future (SSP5): a) percent of CONUS that is classified as a given land-use type. "Dominant" indicates that the percent is taken using grid boxes that are categorized as dominantly that type in WRF only while the "total" amounts give the percent of a land-use type over all of CONUS using fractional land-use fields. b) Mean differences in JJA and DJF for precipitation (precip, %) and temperature (temp, °C) for CONUS or land area that is

dominantly urban or crop, as indicated. For "noLUC-Hist", the mean change from the historical period to the future no-LUC scenario is given as an absolute change for temperature and as a percent change for precipitation. For the other columns, the mean absolute difference in the climate changes between the noted scenarios is given. c) As in b), but for all of CONUS with the mean weighted by the fraction of urban or crop land in a given grid box. d) As in b), but for the percent of land area where the difference is positive. e) As in d), but for all of CONUS with the percent total weighted by the fraction of the land-use type in a given grid box. In b-e), the land-use field used in calculating the urban and crop area means and percent coverages is that of the first listed scenario in the difference.

a)	Hist & noLUC	SSP3	SSP5
Dominant Urban	0.45	0.65	3.24
Total Urban	0.90	1.58	5.64
Domiant Crop	14.12	23.38	15.21
Total Crop	14.63	32.72	18.28
Dominant Pasture	15.59	14.33	14.86
Total Pasture	15.88	12.68	15.11

b)	Urban				Crop				CONUS			
	noLUC-Hist	SSP3-noLUC	SSP5-noLUC	SSP5-SSP3	noLUC-Hist	SSP3-noLUC	SSP5-noLUC	SSP3-SSP5	noLUC-Hist	SSP3-noLUC	SSP5-noLUC	SSP5-SSP3
JJA Precip (%)	15.60	11.17	26.46	25.32	11.30	-0.16	-2.82	0.39	5.41	0.56	-0.49	-1.05
DJF Precip (%)	28.64	1.77	1.35	0.75	24.54	0.31	0.32	-0.25	21.99	0.56	0.45	-0.11
JJA Temp (°C)	4.14	0.79	2.92	2.86	4.27	-0.14	0.18	-0.51	4.38	-0.02	0.25	0.27
DJF Temp (°C)	4.68	0.44	1.27	1.22	5.28	-0.11	0.10	-0.30	4.49	0.03	0.16	0.14

c)	Urban				Crop			
	noLUC-Hist	SSP3-noLUC	SSP5-noLUC	SSP5-SSP3	noLUC-Hist	SSP3-noLUC	SSP5-noLUC	SSP3-SSP5
JJA Precip (%)	8.17	0.56	4.20	4.50	10.97	0.48	-1.39	1.27
DJF Precip (%)	24.72	0.52	0.38	-0.13	24.62	0.58	0.54	0.11
JJA Temp (°C)	4.16	0.05	1.18	1.20	4.28	0.04	0.23	-0.32
DJF Temp (°C)	4.54	0.05	0.54	0.52	5.16	0.00	0.15	-0.17

d)	Urban				Crop				CONUS			
	noLUC-Hist	SSP3-noLUC	SSP5-noLUC	SSP5-SSP3	noLUC-Hist	SSP3-noLUC	SSP5-noLUC	SSP3-SSP5	noLUC-Hist	SSP3-noLUC	SSP5-noLUC	SSP5-SSP3
JJA Precip (%)	91.07	58.75	81.16	77.64	88.82	53.20	28.75	66.92	64.40	60.25	44.79	34.91
DJF Precip (%)	96.43	73.75	60.05	50.50	92.80	58.74	57.66	48.82	90.73	60.76	58.81	46.72
JJA Temp (%)	100.00	57.50	98.74	98.74	100.00	30.57	91.54	1.74	100.00	56.93	96.45	98.16
DJF Temp (%)	100.00	85.00	100.00	99.50	100.00	15.00	87.31	8.74	100.00	75.61	95.57	80.38

e)	Urban				Crop			
	noLUC-Hist	SSP3-noLUC	SSP5-noLUC	SSP5-SSP3	noLUC-Hist	SSP3-noLUC	SSP5-noLUC	SSP3-SSP5
JJA Precip (%)	71.54	51.51	44.31	42.45	85.96	59.74	35.79	68.29
DJF Precip (%)	95.19	62.46	55.80	42.75	92.54	61.70	61.05	53.15
JJA Temp (%)	100.00	35.88	96.66	98.65	100.00	49.49	95.38	1.58
DJF Temp (%)	100.00	64.19	96.84	96.90	100.00	69.87	92.38	15.84

2.4 Analysis Methodology

Statistical significance of the climate change projections and the differences across the projections is tested at the 0.1 level using bootstrapping with bias correction and acceleration and 10,000 bootstrap samples (Efron & Tibshirani, 1993; von Storch & Zwiers, 1999). This method provides an estimate of where the differences are outside of the variability present in the range of years used in the analysis with 90% confidence.

3 Results

3.1 Impact of LUC on Temperature Projections

Temperature projections from our MPI-ESM-LR-driven WRF simulations for most of CONUS range from about 3-6°C in the annual mean, 3-7.5°C in DJF, and 3.5-4.5°C in JJA without LUC (Figure 4). Projected increases are greatest in the Upper Midwest, particularly in DJF, and the Interior West, particularly in JJA. With SSP3-based LUC applied, projected warming decreases by 0.25-1.0°C, over a region stretching from the southern Texas-Louisiana border through Arkansas and into Missouri, regardless of season (Figure 4 and Figure 5). Similar areas of noticeably cooler projections are also scattered throughout the rest of the Southeast U.S. and occasionally in the Western U.S. These significantly cooler projections are strongly tied to locations where the dominant land-use category at a grid box in WRF changed from a forest type to cropland to accommodate the large increases in cropland in SSP3 (cf. Figure 2 and Figure 5). In JJA, the cooling effect of deforestation is most pronounced where deciduous broadleaf forest was replaced with cropland, and in DJF, where evergreen needleleaf forest was replaced. However, the cooling effect over future dominant-cropland-category area in general is only about -0.14 - -0.11°C when averaged across CONUS, although it is widespread, influencing about 16-20% (JJA-DJF, respectively) of CONUS land area (Table 2). Conversely, the scattering of points across the Western U.S. that are 0.25-0.75°C warmer in Figure 5 are coincident with grid boxes that changed from dominantly grassland/pasture to a forest type in WRF due to the decrease in pasture in SSP3. The urban land increase in SSP3+RCP8.5 is small, and so is its overall effect (Table 2), but over some urbanized points in Figure 5 projected temperatures are around 1-3.5°C warmer than in the no-LUC simulations.

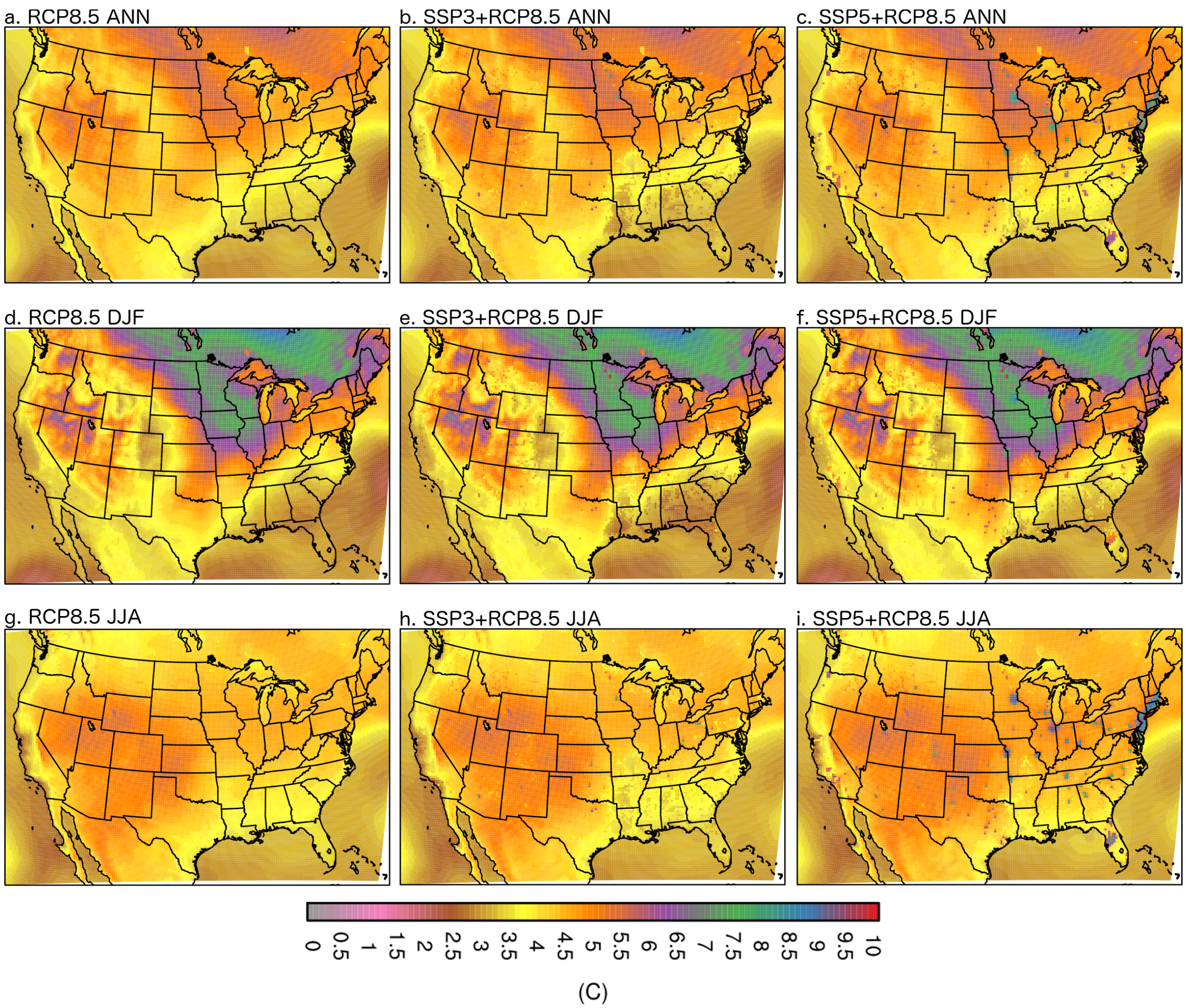

Figure 4. Change in average near-surface temperature from 1980-2005 to 2075-2100 for the no-LUC future scenario (a, d, and g), the SSP3-based LUC scenario (g, e, h), and the SSP5-based LUC scenario (c, f, i). a-c) Annual mean change, d-f) DJF mean change, g-i) JJA mean change. Projections at all points are statistically significant at the 0.1 level, so no indicator of significance was used in this figure.

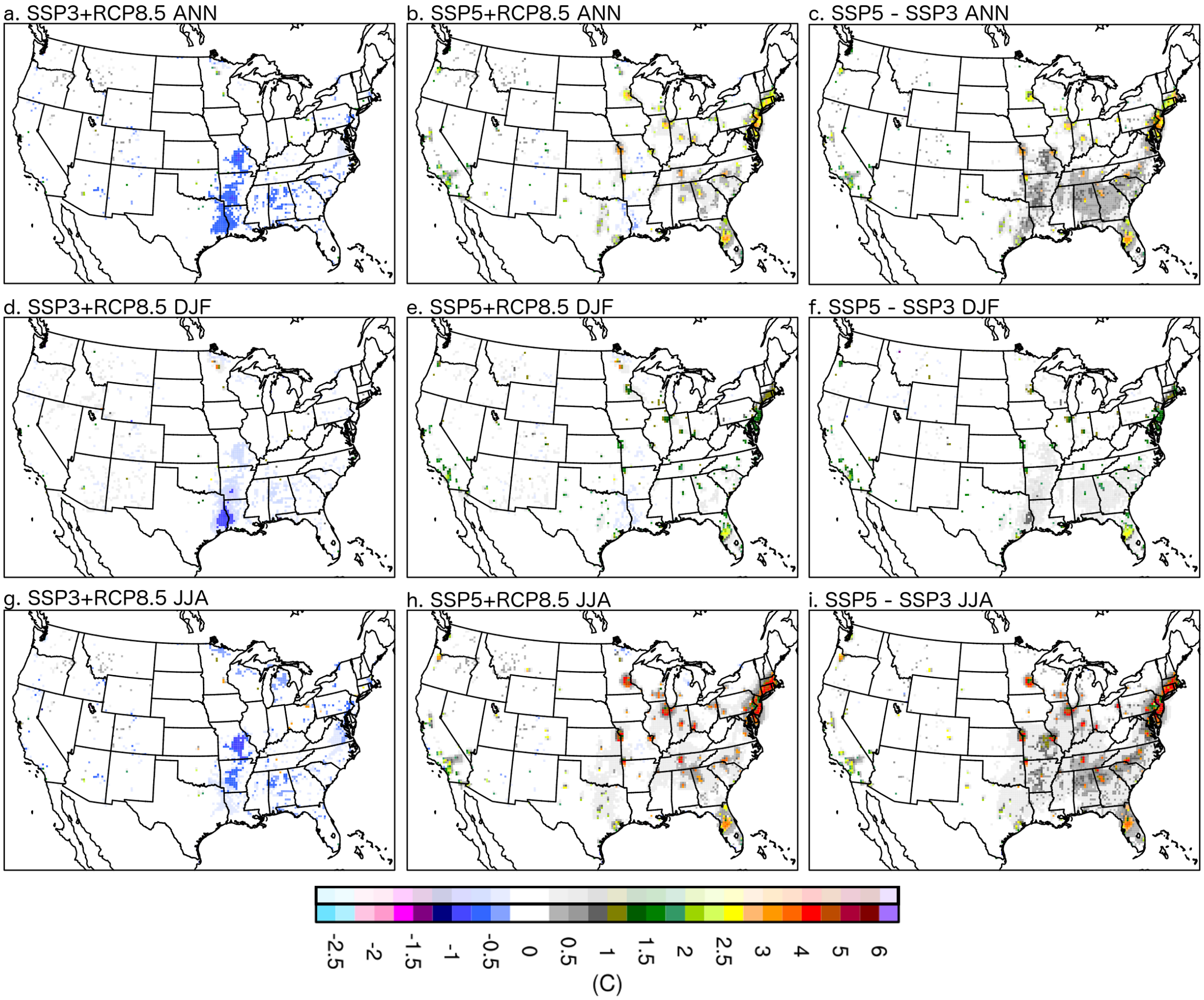

Figure 5. Difference in average near-surface temperature projections between the SSP-based scenarios (left column: SSP3+RCP8.5, right column: SSP5+RCP8.5) and the no-LUC future scenario. a-b) Annual mean difference, c-d DJF mean difference, e-f) JJA mean difference. Differences that are statistically significant at the 0.1 level *and* grid cells where the significance changed between the projections follow the lower colorbar, points that are not significant follow the faded upper colorbar.

The most notable and significant differences in the projections from SSP5+RCP8.5 versus the future without land-use change are the regions of additional warming of 0.5°C up to about 4°C in the annual mean, to 1.5-2.75°C depending on region in winter, to upwards of 4.5°C in summer (Figure 5). This additional projected warming is strongly tied to areas of urbanization in SSP5, but unlike the most significant changes in SSP3, the additional warming projected in SSP5+RCP8.5 expands beyond just the grid boxes that change to a dominantly urban land-use category over a greater region (cf. Figure 2 and Figure 3). Overall in SSP5+RCP8.5, the LUCs, and predominantly the larger urbanization effect, increase CONUS mean temperature projections by 0.16-0.25°C (DJF-JJA), where in SSP3+RCP8.5 the total LUC effect on CONUS mean temperature projections is only around -0.02-0.03°C (JJA-DJF), even though total urban land in SSP5+RCP8.5 accounts for only 5.64% of CONUS land area (a 4.74% increase over the historical LU) and total cropland in SSP3+RCP8.5 accounts for 32.72% of CONUS land area (a 18.09% increase over the historical LU; Table 2 In the end, projections are warmer in SSP5+RCP8.5 than in SSP3+RCP8.5 over almost all of CONUS (Table 2d), although the differences between the scenarios are greatest across the Eastern U.S. (Figure 5). Some of the projection differences noted for SSP3+RCP8.5, where the climate change induced warming is decreased, also apply in SSP5+RCP8.5, but to a lesser extent, as the LUCs in crop and pasture are less extensive (Figure 5). For instance, a decrease in projected warming is still evident near the Texas-Louisiana border, where cropland has replaced forest as the dominant land-category in WRF.

The differences between the near-surface temperature projections from the SSP3+RCP8.5 scenario and the future with no-LUC are likely predominantly due to albedo changes and changes in the partitioning of turbulent heat fluxes. These were shown to be the predominant causes of warming due to afforestation in Davin et al. (2019) across an ensemble of 9 RCMs over Europe, that included a few WRF members, and the predominant causes of cooling due to deforestation across seven coupled global atmosphere-land models in de Noblet-Ducoudré et al. (2012) over North America and Eurasia. Here we likely have similarly influential processes from the Texas-Louisiana border region into Missouri, where warming due to GHG-induced climate change is countered by cooling via deforestation for crop land. Notably, cropland has a higher albedo than forest, which promotes cooler daytime temperatures. Additionally, in JJA in particular, maximum temperature is reduced most where the deciduous forest cover is reduced, and this is additionally coincident with where latent heating is increased and sensible is decreased, while further south, where needleleaf forest is reduced and the effect on temperature is smaller, sensible heating is increased and latent reduced (not shown). Surface roughness may also be playing a role in the cooler projections over the deforested land, as minimum temperature is reduced where forest is reduced for cropland as well (Figure 6). This may be because deforested, lower roughness length land cools more than forested land at night as the stable conditions trap more cool air at the surface, whereas the increased turbulence over forest causes more mixing (Lee et al., 2011).

Differences in projected temperature due to urbanization, particularly in SSP5+RCP8.5 are also likely predominantly due to albedo differences and changes in the partitioning of turbulent heat fluxes. Urbanization notably lowers albedo and causes increased sensible and decreased latent heating, and warmer daytime and nighttime temperatures as a result, as noted in many previous studies of the urban heat island effect (e.g., Arnfield, 2003; Janković & Hebbert, 2012; Masson, 2006). Overall, the effect on minimum temperature is larger than the effect on maximum temperature, as illustrated in Figure 6 for DJF and JJA. This was also seen in Argüeso et al. (2014). For either minimum or maximum temperature in JJA, the additional warming over urban centers due to urbanization alone is on par with the warming due to GHG-induced climate change alone. The same is generally not true in DJF over much of the U.S., except with minimum temperature in FL.

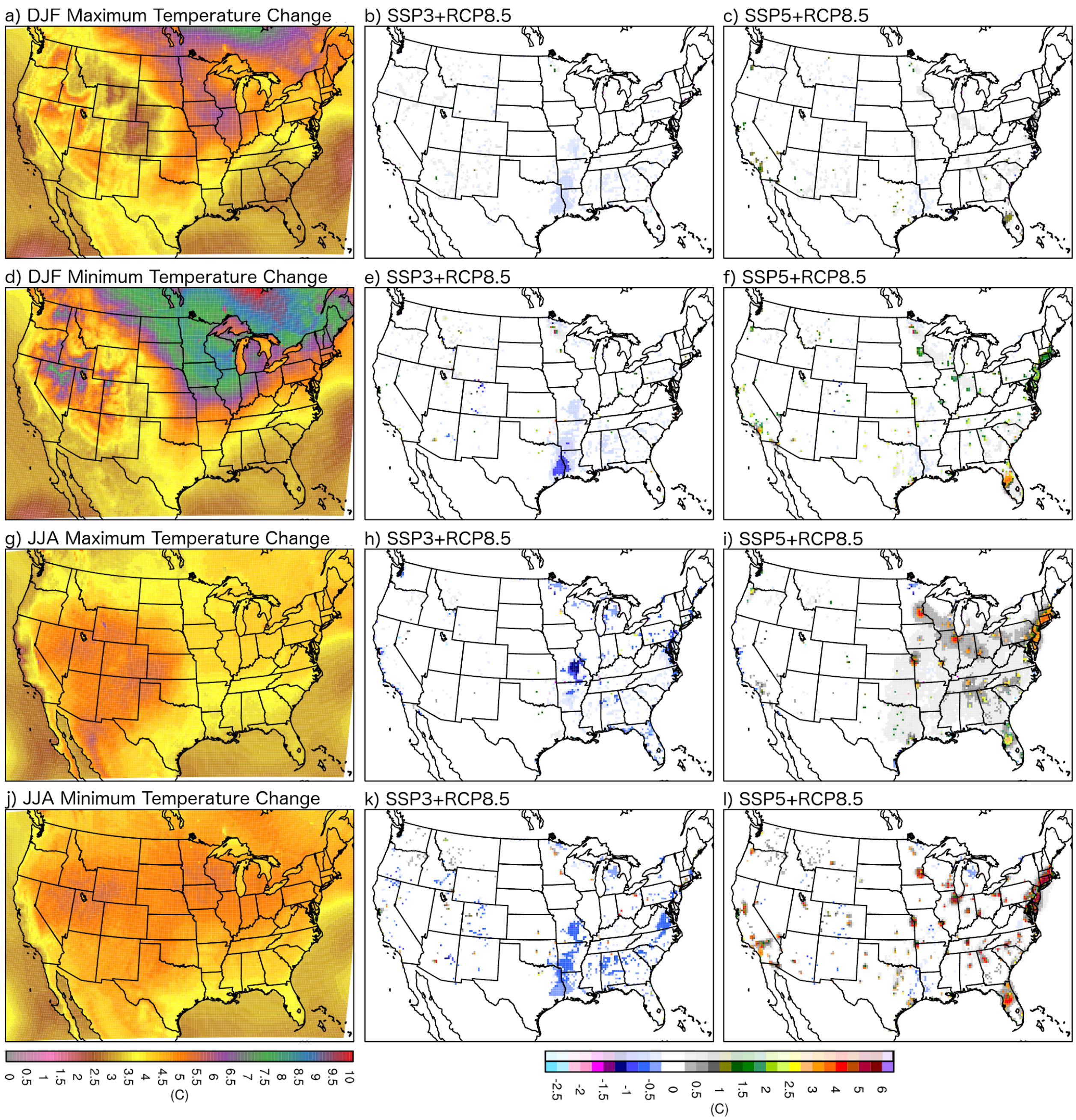

Figure 6. Left column (a, d, g, and j): change in DJF and JJA average near-surface maximum and minimum temperature from 1980-2005 to 2075-2100 for the no-LUC future scenario (as labeled). Projections at all points are statistically significant at the 0.1 level in this column, so no indicator of significance was used. Center column (b, e, h, k): Difference in average near-surface minimum and maximum temperature projections between the SSP3-based scenarios and the no-LUC future scenario. Differences that are statistically significant *and* grid cells where the significance changed between the projections follow the lower colorbar, points that are not significant follow the faded upper colorbar. Right column (c, f, i, l): as in the center column, but

for the SSP5-based scenarios. a-c) DJF maximum temperature; d-f) DJF minimum temperature; g-i) JJA maximum temperature; j-l) JJA minimum temperature.

3.2 Impact of LUC on Precipitation Projections

Annual mean precipitation is projected to increase over much of CONUS north of about 40°N and over parts of the Southeast U.S., while drying is projected for the Southwest (Figure 7). The same is true during winter, but with a greater magnitude increase. In summer, precipitation is projected to strongly decrease over parts of the Southwest U.S, and projections for an increase in precipitation are more limited to Northcentral and Northwest CONUS. Although these projections are from one RCM simulation driven by one GCM, they are consistent with the projections from the full collection of GCMs in CMIP5 (Wuebbles et al., 2017), and generally in agreement with the rest of the NA-CORDEX ensemble (Bukovsky & Mearns, 2020). With SSP3-based LUC applied, the precipitation projections change little (Figure 7, Figure 8, and Table 2). However, there are patterns in the projection difference field that do align with land-use changes in JJA that are worth noting. In the Northwest U.S., for instance, projections for increased precipitation in Southern Idaho and westward from there are enhanced in areas of strong irrigated and dryland crop increases in SSP3 that occur at the expense of shrubland. Additionally, the widespread region of deforestation for cropland that occurs from the southern Texas-Louisiana border north into Missouri in SSP3 has general, insignificant increases in precipitation projected until this LUC is applied, at which point it switches to general, insignificant decreases in precipitation. Although statistically insignificant, the magnitude of this shift (5-15%) is noteworthy and potentially of practical significance since the sign of the projection changed (from an increase to a decrease), and the spatial extent of the effect is widespread. Comparing precipitation characteristics from the point in Figure 3 in Arkansas that experiences increased crop fraction under SSP3+RCP8.5 versus the one just to its east that does not and the no-LUC future simulation, indicates that this is due to a much smaller increase in the intensity of precipitation over the region of increased cropland compared to the point downstream and compared to the same point in the no-LUC future (not shown). This interacts with a decrease in the frequency of future precipitation at these points that is much more similar between the two future projections and between the two points (not shown).

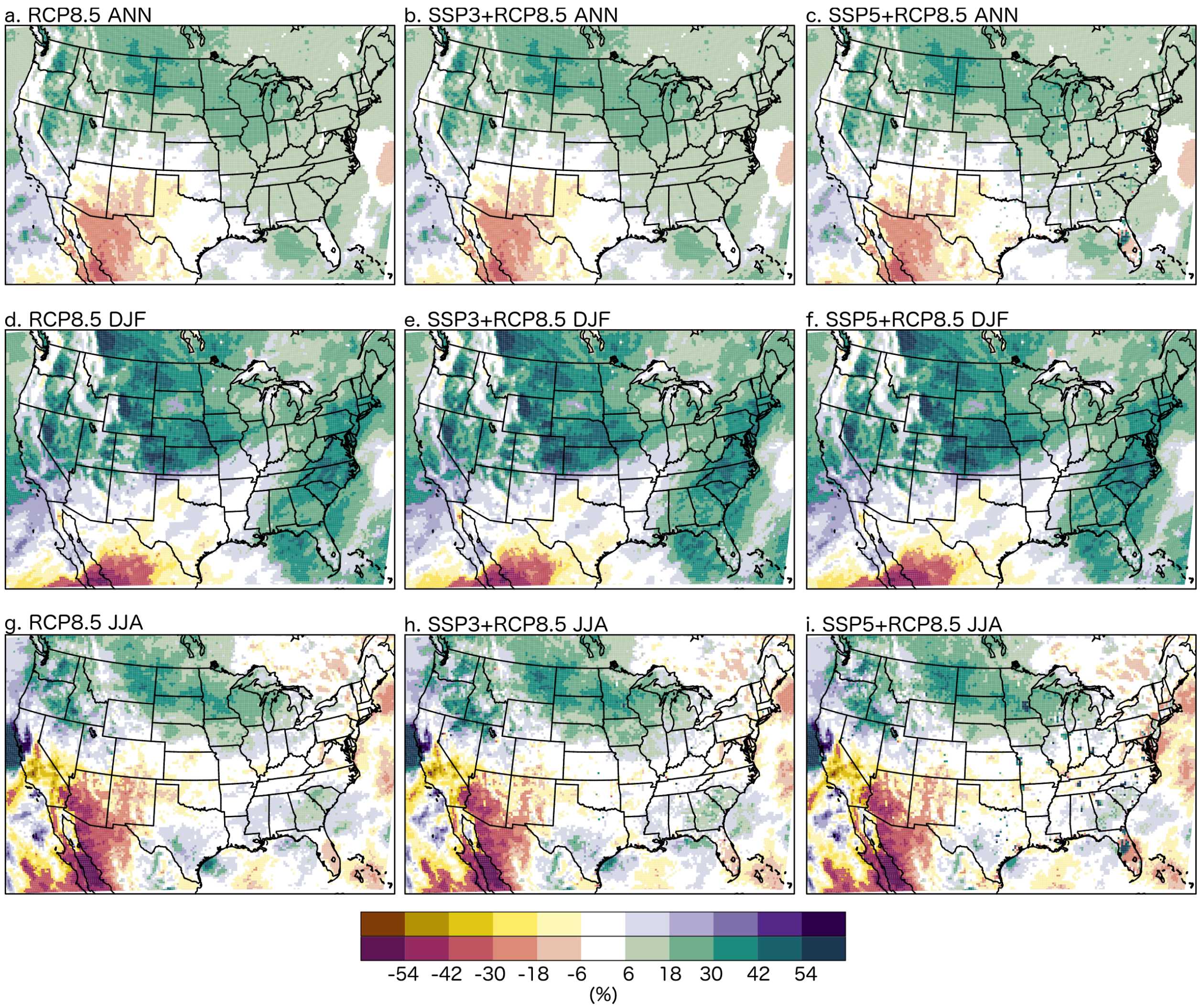

Figure 7. As in Figure 4, but for the percent change in mean precipitation. Differences that are statistically significant at the 0.1 level *and* grid cells where the significance changed between the projections follow the lower colorbar, points that are not significant follow the faded upper colorbar.

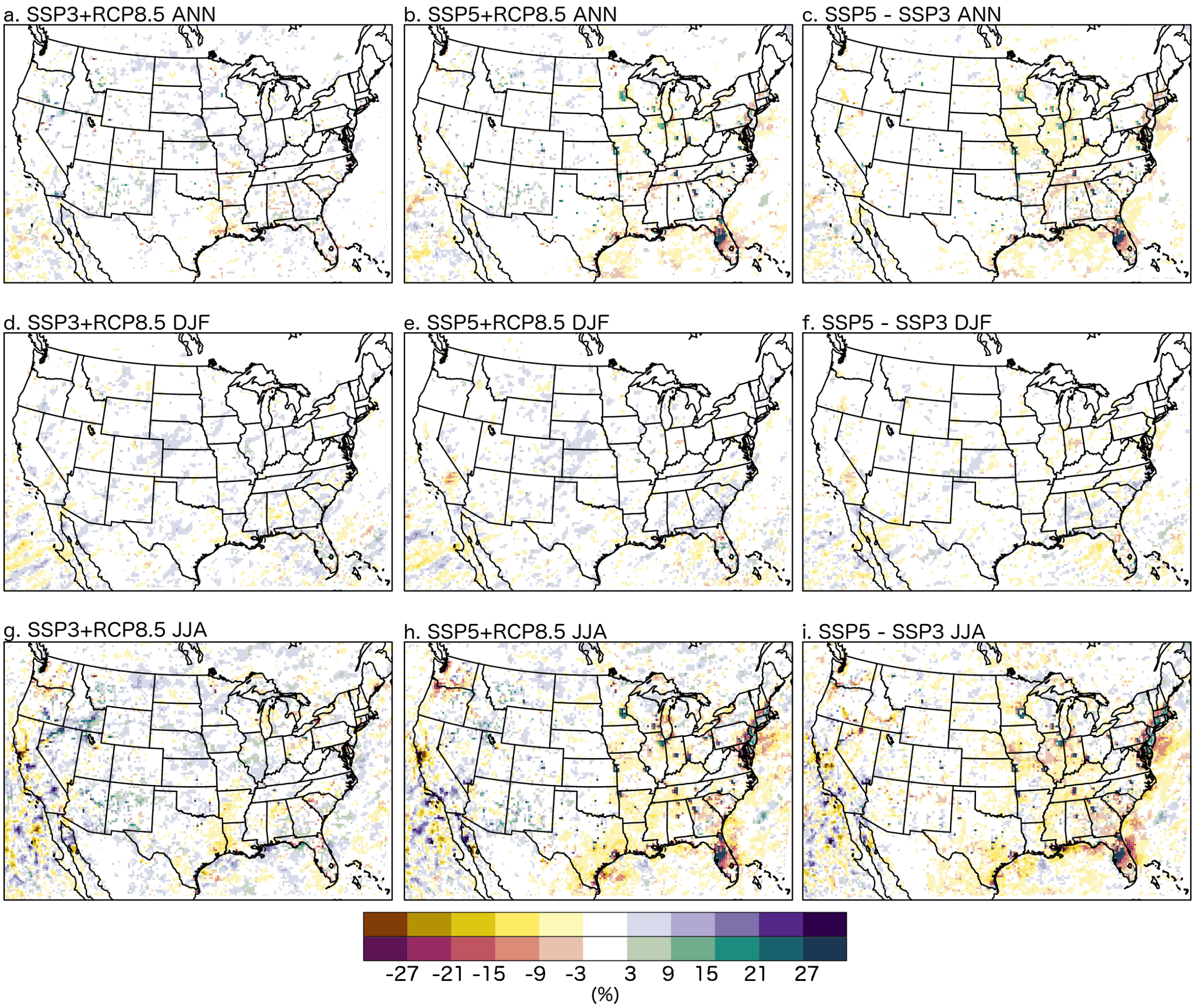

Figure 8. As in Figure 5, but for the absolute difference in the average precipitation percent change projections. Differences that are statistically significant at the 0.1 level *and* grid cells where the significance changed between the projections follow the lower colorbar, points that are not significant follow the faded upper colorbar.

The differences between the no-LUC precipitation projections and the SSP5-based LUC projections are stronger and more noteworthy than those that occur when the SSP3-based LUC is applied in the future climate, particularly during the warm season (including JJA) over the eastern half of CONUS (Figure 7 and Figure 8). Significant increases in precipitation occur over areas that experience urbanization in SSP5+RCP8.5 in the eastern U.S., particularly in areas that become dominantly urban, and precipitation projections are decreased in the surrounding areas, especially downstream from the urbanized areas. The same does happen under SSP3+RCP8.5, but to a much lesser extent given the much smaller increase in urban coverage. On the other hand, over areas of urban expansion on the West Coast (i.e., near San Francisco, Portland, and Seattle), there is a reduction in precipitation in the SSP5+RCP8.5 scenario in JJA compared to the no-LUC future scenario, but JJA is already the dry season for those areas. Overall, the CONUS mean precipitation change in SSP5+RCP8.5 is drier than SSP3+RCP8.5 by about 1% in the absolute sense; however, that 1% is a 17% change relative to the no-LUC scenario (i.e., when viewed as a percent difference) (Table 2, Figure 8). It is also drier over about 65% of the country because of the widespread drying around urban areas, despite having considerably more precipitation over the dominantly urban points in this scenario. Considering that LUCs under SSP3 are primarily agricultural and SSP5 primarily urban, these results suggest that urban land expansion is potentially more influential than cropland expansion on future precipitation patterns in North America.

Differences in the projections of precipitation characteristics from SSP5+RCP8.5 and the no-LUC scenario for the points targeting urban areas in Figure 3 are summarized in Table 3. These differences indicate that the stronger increase in mean precipitation over Eastern U.S. urbanized areas in the future in JJA is associated with, in all locations, a greater increase in precipitation intensity (as intensity is projected to increase in all locations - not shown) and longer precipitation events. Differences in precipitation frequency projections are mixed depending on location, but frequency is projected to decrease at all locations except PDX in the no-LUC scenario initially. The sign of the frequency projection switches following the application of the SSP5+RCP8.5 LUCs in DFW, FL, and PDX. Intensity projections in the SSP5+RCP8.5 projections at the "rural" points downstream of the urbanized areas are still greater than in the no-LUC projections, but to a much lesser extent than at the "urban" points. The rural points in the SSP5+RCP8.5 projections all have less frequent precipitation than the no-LUC scenario though, meaning that the projection for decreased frequency in the no-LUC scenario for these points decreases further. Additionally, many of the rural locations have shorter precipitation events.

Table 3. Absolute differences in JJA average percent changes projected from the baseline for different precipitation characteristics between the SSP5+RCP8.5 projections minus the no-LUC projections for the points indicated in Figure 3 and defined in Section 2.3. a) Points that are directly over the urbanization centers, and b) eastward/downstream points that are more "rural". Precipitation characteristics include average precipitation (Average), precipitation intensity (Intensity), the percent of hours at a point that are either wet (%Wet) or dry (%Dry), and the average number of consecutive wet or dry hours per precipitation event (CWH and CDH, respectively). Wet hours are defined as hours with precipitation greater than 0.01 mm/hr, and all statistics were calculated from hourly precipitation output. As indicated, column averages do not include values from PDX.

a) URBAN	Average (%)	Intensity (%)	%Wet (%)	%Dry (%)	CWH (%)	CDH (%)
CHI	25.44	37.26	-3.18	0.79	8.56	16.46
DFW	41.52	17.94	19.10	-2.10	9.76	-14.15
FL	61.60	33.30	23.31	-6.94	28.51	-2.04
MSP	29.04	51.24	-10.74	2.93	3.23	18.80
NJ	24.65	19.74	7.36	-1.57	7.92	-3.69
PDX	-29.74	7.12	-27.95	5.57	15.42	64.47
Average (no PDX)	36.45	31.90	7.17	-1.38	11.59	3.08

b) RURAL	Average (%)	Intensity (%)	%Wet (%)	%Dry (%)	CWH (%)	CDH (%)
CHI	-9.86	21.46	-17.86	4.57	-5.66	27.02
DFW	-0.51	8.68	-6.14	0.69	-0.57	8.64
FL	-15.51	2.16	-15.31	2.99	-3.70	22.17
MSP	-6.62	22.66	-19.19	5.74	-8.65	16.92
NJ	-9.20	9.62	-10.11	1.36	3.25	34.44
PDX	2.39	7.00	-2.94	0.23	-0.94	2.83
Average (no PDX)	-8.34	12.92	-13.72	3.07	-3.07	21.84

Similar processes are at play in producing the different warm season precipitation projections from the SSP5+RCP8.5 scenario near Eastern U.S. urban areas versus the no-LUC scenario as are seen in observations and modeling studies (e.g., Argüeso et al., 2016; Bornstein & Lin, 2000; Niyogi et al., 2011; Shepherd, 2005; Shepherd & Burian, 2003; Wu et al., 2019). The warming, potentially aided by the increased surface roughness, over the large urbanized areas in the SSP5+RCP8.5 simulations compared to the no-LUC future induces low-level convergence and low-level upward motion (Figure 9a, b). Surface humidity may be lower in the

SSP5+8.5 simulations over the urbanized areas, as expected due to decreased surface evaporation, but the enhanced low-level convergence in the near surface winds leads to increased moisture flux into the urbanized areas (Figure 9c, d). The enhanced surface warming over the urbanized areas also destabilizes the lower atmosphere, as suggested by the lower convective inhibition (Figure 9e). The lifting condensation level and level of free convection are also higher over the heavily urbanized regions, but so too is the boundary layer height, presumably allowing these levels to be reached more often (Figure 9f-h). All of the above translates into enhanced precipitation over all of the urbanized areas in the form of higher intensity storms and storms that persist for longer. It does not translate to more frequent precipitation than in the no-LUC future in all cities though, despite a slight diurnal enhancement in the frequency of precipitation in the late-afternoon/early evening in the Eastern U.S. cities examined, excluding FL (not shown). In the less urbanized surroundings, conditions are made less favorable for precipitation. This is generally best represented by the stronger low-level divergence of the near-surface winds outside of the heavily urbanized areas and broad areas of increased convective inhibition across the Eastern U.S., that then leads to fewer and often shorter precipitation events. Near coastal regions, the large urbanized areas and their intense heat island effect also interact with and enhance the sea-breeze. In Florida, this effect is strong enough to lead to a nearly permanent sea-breeze throughout the future mean JJA diurnal cycle, as the land does not always cool down to less than the surrounding water temperatures at night, although the contrast between land and water does decrease overnight (not shown). This is not the case in the expanded Northeast Megalopolis.

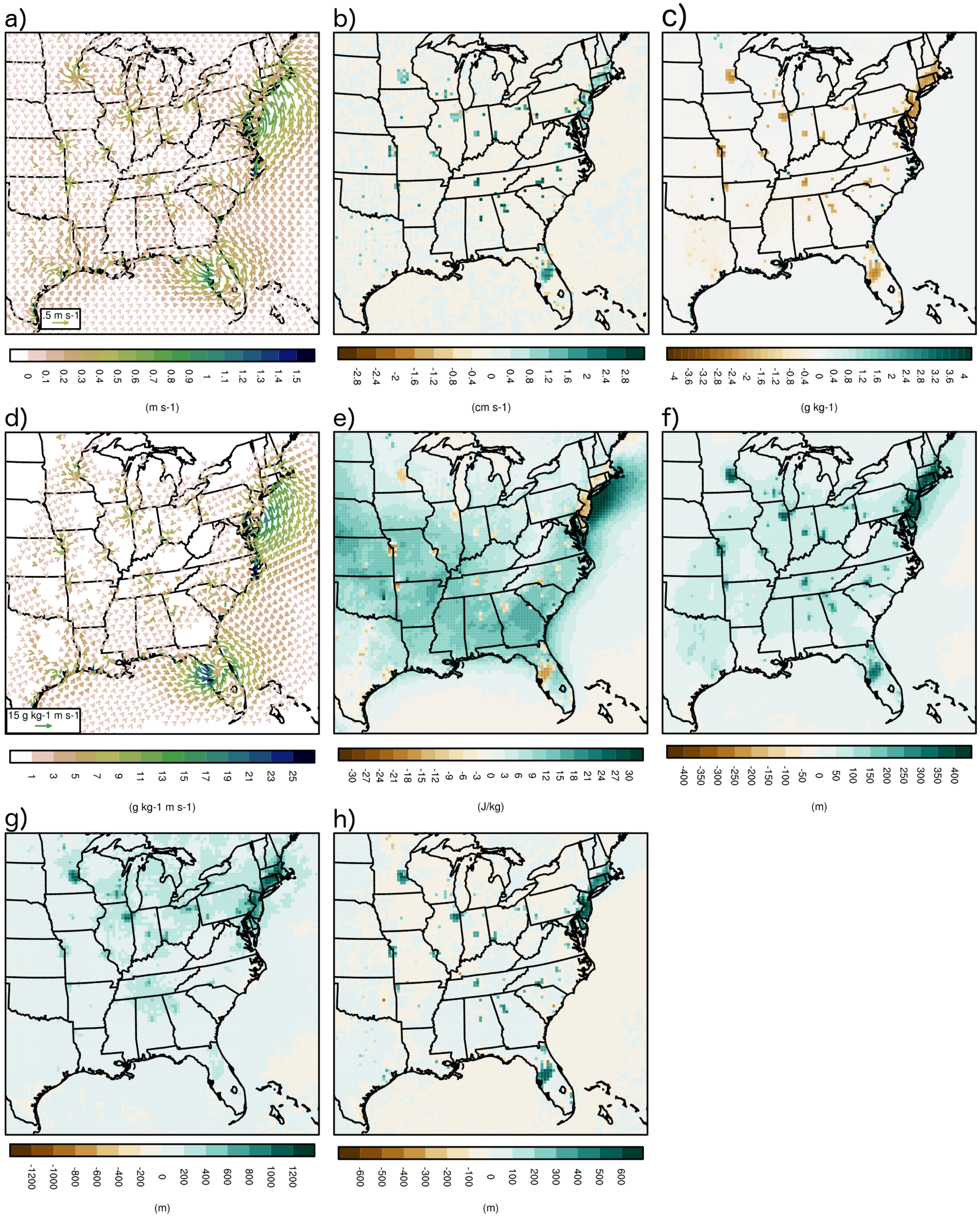

Figure 9. JJA absolute difference between projections using the SSP5+RCP8.5 scenario and no-LUC future scenario for a) near-surface wind, b) 850-hPa vertical velocity, c) near-surface specific humidity, d) near-surface moisture flux, e) convective inhibition, f) lifting condensation level, g) level of free convection, h) boundary layer height.

4 Summary and Discussion

Simulations were performed to examine how not including the land-use change that underlies the SSP-RCP framework may affect regional climate model projections of future climate change performed for CORDEX to date. Focusing on the effects on mean temperature and precipitation, we have found that regional climate change projections are sensitive to SSP-based urban and agricultural land-use changes, as evidenced by statistically significant differences in the projections in some regions. We have also shown that the type of land-use change that is assumed matters (i.e. SSP3 vs. SSP5), a conclusion relevant to the scenarios framework.

In regions of significant crop expansion like the Southeast U.S., particularly in SSP3+RCP8.5, projected temperature increases are dampened by 0.5-1.5℃. In localities with large future urbanization projections, projected temperature increases are substantially magnified in and beyond urban boundaries. Projections for mean temperature are up to 4-5℃ greater in JJA in urban centers. The additional warming over urban centers due to urbanization alone is on par with the warming due to GHG-forced climate change alone. This is also the case for both minimum and maximum temperature in JJA under SSP5+RCP8.5. In SSP5+RCP8.5 this additional warming is not limited to urban centers; projected temperature increases are up to 0.25-0.75 ℃ greater between them in the eastern half of the U.S. in JJA. While regional precipitation is not greatly influenced by land-use change in SSP3+RCP8.5, in SSP5+RCP8.5 over urbanized areas, mean precipitation is considerably enhanced, mostly due to an increase in the intensity of the events, but also an increase in the length of the events. This has potential implications for projections of socio-environmental challenges like urban flooding. Precipitation is also suppressed around the urbanized areas.

Overall, the differences between the projections from the SSP-based LUC scenarios suggests that urban land expansion is potentially more influential than cropland expansion on CONUS temperature and precipitation projections, at least under RCP8.5.

These projections, however, only come from one RCM configuration forced by one GCM under one RCP and two future SSPs. They demonstrate that the CORDEX projections can be significantly affected by including LUCs underlying the SSP+RCP framework. However, more research is needed to document the effect RCM+LUC sensitivities and structural uncertainties have on the projections across different LUC scenarios.

For example, as we leveraged NA-CORDEX simulations here, and were constrained by the existing WRF configuration, changing some relevant model options may be worth exploring in future studies. For instance, here the urban environment is simply represented by differences in land surface cover properties, and not an urban canopy model. Therefore, the three-dimensional nature of cities is not represented. Using an urban canopy model would likely provide more realistic simulations. Additionally, the land-surface parameterization used had no option for considering sub-grid scale fractional land cover at the time the CORDEX simulations were produced. It does now, and so do other land-surface schemes. Considering only the dominant land-cover type in a grid box may have caused an under- and/or over-estimation of the effect of the LUC on the projections, it likely also altered the intended amount of LUC applied relative to that projected by the land-use models and implemented in the fractional land-use fields. We hope to examine how these modeling choices affected our results in future work. However, results from this study are broadly consistent with observations and other modeling studies that have examined the role of LUC on climate in terms of their trend and broad physical effect, as discussed previously in the context of the results. Nonetheless, the resolution in this study is also potentially too coarse for some urbanization effects with or without the use of an urban parameterization as well (e.g. the 50-75km downstream influence of the urban canopy on precipitation seen, for instance, in Niyogi et al. (2011)), and a higher resolution would likely provide a better representation of warm-season precipitation, in particular, regardless of proximity to an urban area. Furthermore, the effect of urbanization on the precipitation projections here does not include any changes in anthropogenic aerosols and, therefore, does not consider their effect on nucleation. We also do not consider added anthropogenic heat. Likewise, urban land change considers only the expansion of urban extent. An enhanced dataset of changes in urban morphological characteristics would be more realistic, but is not currently available.

Our methods for applying the LUCs in WRF may also warrant additional study. For example, while we tested different methods for applying the crop projections from the LUM to the different crop types in WRF, we did not examine our application of pasture projections with as much scrutiny. In the future we will experiment with applying the changes to other categories that could be considered pasture, not just grassland. Pasture projections in this case though do not have as widespread an effect on climate as the crop and urban projections.

Ultimately, this work suggests that for a more complete exploration of uncertainty in future regional climate projections, the regional modeling community should consider the land-use changes that underlie the SSP+RCP framework, and not just the GHG concentration scenarios. This is particularly true as the community looks forward to downscaling simulations from CMIP6 ScenarioMIP (O'Neill et al., 2016). Such analyses, however, would require that sub-national land-use change scenarios that are consistent with all relevant SSP+RCP scenarios be available at near the resolution of the models over, preferably, the full region of interest. As there are many different methods in which the LUC can be incorporated into the RCMs and many different ways in which the land surface can be represented in RCMs, additional sensitivity tests should be performed, like those being produced for LUCAS (Davin et al., 2019) in Europe, and groups which undertake LUC incorporation in their projections should fully document their methods. Finally, the CORDEX community should discuss modeling strategies and methodology for the use of SSP-based LUC scenarios to establish best-practices.

Acknowledgements & Data

The authors would like to thank the modeling teams that contributed to NA-CORDEX (Mearns et al., 2017). Archiving of NA-CORDEX data was funded by the U.S. Department of Defense's Environmental Security Technology Certification Program. NA-CORDEX data is available via na-cordex.org. Derived data that is essential to reproducing the analysis shown herein that is not publicly available through NA-CORDEX, including the LUC scenario simulation data, is available via [*dataset and DOI creation is in progress, and will be published before manuscript publication through NCAR's DASH*]. We also acknowledge high-performance computing support provided by NCAR's Computational and Information Systems Laboratory (Computational And Information Systems Laboratory, 2017), and NCL (Brown et al., 2012). This research was produced as a part of the Framework for Assessing Climate's Energy-Water-Land nexus by Targeted Simulations (FACETS) project, which is supported by the U.S. Department of Energy's Regional and Global Climate Modeling program via grant DE-SC0016438. Additional support was provided by the Regional Climate Uncertainty Program, managed by Dr. Mearns, funded by NSF under the NCAR cooperative agreement. Dr. Mearns was funded by NCAR, which is funded by the NSF.

References

Argüeso, D., Di Luca, A., & Evans, J. P. (2016). Precipitation over urban areas in the western Maritime Continent using a convection-permitting model. *Climate Dynamics*, *47*(3), 1143–1159. https://doi.org/10.1007/s00382-015-2893-6

Argüeso, D., Evans, J. P., Fita, L., & Bormann, K. J. (2014). Temperature response to future urbanization and climate change. *Climate Dynamics*, *42*(7), 2183–2199. https://doi.org/10.1007/s00382-013-1789-6

Arnfield, A. J. (2003). Two decades of urban climate research: a review of turbulence, exchanges of energy and water, and the urban heat island. *International Journal of Climatology*, *23*(1), 1–26. https://doi.org/10.1002/joc.859

Belušić, D., Fuentes-Franco, R., Strandberg, G., & Jukimenko, A. (2019). Afforestation reduces cyclone intensity and precipitation extremes over Europe. *Environmental Research Letters* 14(7), 074009. https://doi.org/10.1088/1748-9326/ab23b2

Berckmans, J., Hamdi, R., & Dendoncker, N. (2019). Bridging the Gap Between Policy-Driven Land Use Changes and Regional Climate Projections. *Journal of Geophysical Research, D: Atmospheres*, *124*(12), 5934–5950. https://doi.org/10.1029/2018JD029207

Bornstein, R., & Lin, Q. (2000). Urban heat islands and summertime convective thunderstorms in Atlanta: three case studies. *Atmospheric Environment*, 34(3), 507–516. https://doi.org/10.1016/s1352-2310(99)00374-x

Brown, D., Brownrigg, R., Haley, M., & Huang, W. (2012). *NCAR Command Language (NCL)*. UCAR/NCAR - Computational and Information Systems Laboratory (CISL). https://doi.org/10.5065/D6WD3XH5

Bukovsky, M. S., & Mearns, L. O. (2020). Regional Climate Change Projections from NA-CORDEX and their Relation to Climate Sensitivity. *Climatic Change*, *Accepted*, In Press. https://doi.org/10.1007/s10584-020-02835-x

Computational And Information Systems Laboratory. (2017). *Cheyenne: SGI ICE XA Cluster*. UCAR/NCAR. https://doi.org/10.5065/D6RX99HX

Davin, E. L., Rechid, D., Breil, M., Cardoso, R. M., Coppola, E., Hoffmann, P., ... & Raffa, M. (2020). Biogeophysical impacts of forestation in Europe: first results from the LUCAS (Land Use and Climate Across Scales) regional climate model intercomparison. Earth System Dynamics, 11(1), 183-200. https://doi.org/10.5194/esd-11-183-2020 de Noblet-Ducoudré, N., Boisier, J.-P., Pitman, A., Bonan, G. B., Brovkin, V., Cruz, F., Delire, C., Gayler, V., van den Hurk B. J. J. M., Lawrence, P. J., van der Molen, M. K., Müller, C., Reick, C. H., Strengers, B. J., & Voldoire, A. (2012). Determining Robust Impacts of Land-Use-Induced Land Cover Changes on Surface Climate over North America and Eurasia: Results from the First Set of LUCID Experiments. *Journal of Climate*, *25*(9), 3261–3281. https://doi.org/10.1175/JCLI-D-11-00338.1

Efron, B., & Tibshirani, R. (1993). *An introduction to the bootstrap*. Chapman and Hall/CRC.

Gálos, B., Mátyás, C., & Jacob, D. (2011). Regional characteristics of climate change altering effects of afforestation. *Environmental Research Letters*, *6*(4), 044010. https://doi.org/10.1088/1748-9326/6/4/044010

Gao, J., & O'Neill, B. C. (2019). Data-driven spatial modeling of global long-term urban land development: The SELECT model. *Environmental Modelling & Software*, *119*, 458–471. https://doi.org/10.1016/j.envsoft.2019.06.015

Gao, J., & O'Neill, B. C. (2020). Mapping global urban land for the 21st century with data-driven simulations and Shared Socioeconomic Pathways. *Nature Communications*, *11*(1), 2302. https://doi.org/10.1038/s41467-020-15788-7

Harrison, P. A., Dunford, R. W., Holman, I. P., Cojocaru, G., Madsen, M. S., Chen, P.-Y., Pedde, S., & Sandars, D. (2019). Differences between low-end and high-end climate change impacts in Europe across multiple sectors. *Regional Environmental Change*, *19*(3), 695–709. https://doi.org/10.1007/s10113-018-1352-4

Huber, D. B., Mechem, D. B., & Brunsell, N. A. (2014). The Effects of Great Plains Irrigation on the Surface Energy Balance, Regional Circulation, and Precipitation. *Climate*, *2*(2), 103–128. https://doi.org/10.3390/cli2020103

Janković, V., & Hebbert, M. (2012). Hidden climate change--urban meteorology and the scales of real weather. *Climatic Change*, *113*(1), 23–33. https://doi.org/10.1007/s10584-012-0429-1

Jones, A. D., Collins, W. D., Edmonds, J., Torn, M. S., Janetos, A., Calvin, K. V., Thomson, A., Chini, L. P., Mao, J., Shi, X., Thornton, P., Hurtt, G. C., & Wise, M. (2013). Greenhouse Gas Policy Influences Climate via Direct Effects of Land-Use Change. *Journal of Climate*, *26*(11), 3657–3670. https://doi.org/10.1175/JCLI-D-12-00377.1

Lawrence, D. M., Hurtt, G. C., Arneth, A., Brovkin, V., Calvin, K. V., Jones, A. D., Jones, C. D., Lawrence, P. J., de Noblet-Ducoudré, N., Pongratz, J., Seneviratne, S. I., & Shevliakova, E. (2016). The Land Use Model Intercomparison Project (LUMIP) contribution to CMIP6: rationale and experimental design. *Geoscientific Model Development*, *9*(9), 2973–2998. https://doi.org/10.5194/gmd-9-2973-2016

Lee, X., Goulden, M. L., Hollinger, D. Y., Barr, A., Black, T. A., Bohrer, G., Bracho, R., Drake, B., Goldstein, A., Gu, L., Katul, G., Kolb, T., Law, B. E., Margolis, H., Meyers, T., Monson, R., Munger, W., Oren, R., Paw U, K. T., … Zhao, L. (2011). Observed increase in local cooling effect of deforestation at higher latitudes. *Nature*, *479*(7373), 384–387. https://doi.org/10.1038/nature10588

Masson, V. (2006). Urban surface modeling and the meso-scale impact of cities. *Theoretical and Applied Climatology*, *84*(1-3), 35–45. https://doi.org/10.1007/s00704-005-0142-3

Mearns, L. O., McGinnis, S., Korytina, D., Arritt, R., Biner, S., Bukovsky, M., Chang, H. I., Christensen, O., Herzmann, D., Jiao, Y., & Others. (2017). The NA-CORDEX dataset, version 1.0. *NCAR Climate Data Gateway. Boulder (CO): The North American CORDEX Program*, *10*, D6SJ1JCH.

Meiyappan, P., Dalton, M., O’Neill, B. C., & Jain, A. K. (2014). Spatial modeling of agricultural land use change at global scale. *Ecological Modelling*, *291*, 152–174. https://doi.org/10.1016/j.ecolmodel.2014.07.027

Moss, R. H., Edmonds, J. A., Hibbard, K. A., Manning, M. R., Rose, S. K., van Vuuren, D. P., Carter, T. R., Emori, S., Kainuma, M., Kram, T., Meehl, G. A., Mitchell, J. F. B., Nakicenovic, N., Riahi, K., Smith, S. J., Stouffer, R. J., Thomson, A. M., Weyant, J. P., & Wilbanks, T. J. (2010). The next generation of scenarios for climate change research and assessment. *Nature*, *463*(7282), 747–756. https://doi.org/10.1038/nature08823

Niyogi, D., Pyle, P., Lei, M., Arya, S. P., Kishtawal, C. M., Shepherd, M., Chen, F., & Wolfe, B. (2011). Urban Modification of Thunderstorms: An Observational Storm Climatology and Model Case Study for the Indianapolis Urban Region. *Journal of Applied Meteorology and Climatology*, *50*(5), 1129–1144. https://doi.org/10.1175/2010JAMC1836.1

O’Neill, B. C., Conde, C., Ebi, K., Friedlingstein, P., Fuglestvedt, J., Hasegawa, T., Kok, K., Kriegler, E., Monteith, S., Pichs-Madruga, R., Preston, B., Sillman, J., van Ruijven, B., & van Vuuren, D. (2019). *Forum on Scenarios of Climate and Societal Futures: Meeting Report* (Pardee Center Working Paper 2019.10.04). University of Denver, Denver, CO.

O'Neill, B. C., Kriegler, E., Ebi, K. L., Kemp-Benedict, E., Riahi, K., Rothman, D. S., van Ruijven, B. J., van Vuuren, D. P., Birkmann, J., Kok, K., Levy, M., & Solecki, W. (2017). The roads ahead: Narratives for shared socioeconomic pathways describing world futures in the 21st century. *Global Environmental Change: Human and Policy Dimensions*, *42*, 169–180. https://doi.org/10.1016/j.gloenvcha.2015.01.004

O'Neill, B. C., Tebaldi, C., Van Vuuren, D. P., Eyring, V., Friedlingstein, P., Hurtt, G., Knutti, R., Kriegler, E., Lamarque, J. F., Lowe, J., Meehl, G. A., Moss, R., Riahi, K., & Sanderson, B. M. (2016). *The Scenario Model Intercomparison Project (ScenarioMIP) for CMIP6*. https://doi.org/10.5194/gmd-9-3461-2016

Rendfrey, T., Bukovsky, M. S., & McGinnis, S. (2018). *NA-CORDEX Visualization Collection* [Data set]. UCAR/NCAR. https://doi.org/10.5065/90ZF-H771

Ren, X., Weitzel, M., O'Neill, B. C., Lawrence, P., Meiyappan, P., Levis, S., Balistreri, E. J., & Dalton, M. (2018). Avoided economic impacts of climate change on agriculture: integrating a land surface model (CLM) with a global economic model (iPETS). *Climatic Change*, *146*(3), 517–531. https://doi.org/10.1007/s10584-016-1791-1

Riahi, K., van Vuuren, D. P., Kriegler, E., Edmonds, J., O'Neill, B. C., Fujimori, S., Bauer, N., Calvin, K., Dellink, R., Fricko, O., Lutz, W., Popp, A., Cuaresma, J. C., Kc, S., Leimbach, M., Jiang, L., Kram, T., Rao, S., Emmerling, J., … Tavoni, M. (2017). The Shared Socioeconomic Pathways and their energy, land use, and greenhouse gas emissions implications: An overview. *Global Environmental Change: Human and Policy Dimensions*, *42*, 153–168. https://doi.org/10.1016/j.gloenvcha.2016.05.009

Shepherd, J. M. (2005). A Review of Current Investigations of Urban-Induced Rainfall and Recommendations for the Future. *Earth Interactions*, 9(12), 1–27. https://doi.org/10.1175/ei156.1

Shepherd, J. M., & Burian, S. J. (2003). Detection of Urban-Induced Rainfall Anomalies in a Major Coastal City. *Earth Interactions*, *7*, 1–17. https://doi.org/10.1175/1087-3562(2003)007<0001:DOUIRA>2.0.CO;2

Skamarock, W. C., Klemp, J. B., Dudhia, J., Gill, D. O., Barker, D. M., Wang, W., & Powers, J. G. (2005). *A description of the Advanced Research WRF version 2*.

Tölle, M. H., Breil, M., Radtke, K., & Panitz, H.-J. (2018). Sensitivity of European Temperature to Albedo Parameterization in the Regional Climate Model COSMO-CLM Linked to

Extreme Land Use Changes. *Frontiers of Environmental Science & Engineering in China*, *6*, 123. https://doi.org/10.3389/fenvs.2018.00123

von Storch, H., & Zwiers, F. W. (1999). *Statistical Analysis in Climate Research*. Cambridge University Press.

Wuebbles, D. J., Fahey, D. W., Hibbard, K. A., Arnold, J. R., DeAngelo, B., Doherty, S., Easterling, D. R., Edmonds, J., Edmonds, T., Hall, T., Hayhoe, K., Huffman, F. M., Horton, R., Huntzinger, D., Jewett, L., Knutson, T., Kopp, R. E., Kossin, J. P., Kunkel, K. E., … Walsh, J. (2017). *Climate Science Special Report: Fourth National Climate Assessment (NCA4), Volume I*. https://lib.dr.iastate.edu/agron_reports/8/

Wu, M., Luo, Y., Chen, F., & Wong, W. K. (2019). Observed Link of Extreme Hourly Precipitation Changes to Urbanization over Coastal South China. *Journal of Applied Meteorology and Climatology*, *58*(8), 1799–1819. https://doi.org/10.1175/JAMC-D-18-0284.1

Yilmaz, Y. A., Sen, O. L., & Turuncoglu, U. U. (2019). Modeling the hydroclimatic effects of local land use and land cover changes on the water budget in the upper Euphrates--Tigris basin. *Journal of Hydrology*, *576*, 596–609. https://doi.org/10.1016/j.jhydrol.2019.06.074